Oxidation states in scanning-probe-induced Si_3N_4 to SiO_x conversion studied by scanning photoemission microscopy

R. Klauser[a] and I.-H. Hong
Synchrotron Radiation Research Center, No. 1 R&D Road VI, Hsinchu 300, Taiwan, Republic of China

H.-J. Su, T. T. Chen, and S. Gwo
Department of Physics, National Tsing-Hua University, Hsinchu 300, Taiwan, Republic of China

S.-C. Wang
Institute of Atomic and Molecular Sciences, Academia Sinica, Taipei 106, Taiwan, Republic of China

T. J. Chuang[b]
Center for Condensed Matter Sciences, National Taiwan University, Taipei 106, Taiwan, Republic of China

V. A. Gritsenko
Institute of Semiconductor Physics, Lavrentieva Avenue 13, Novosibirsk 630090, Russia

(Received 29 June 2001; accepted for publication 22 August 2001)

The biased conductive probe of an atomic force microscope can induce local oxidation in ambience for converting silicon nitride films to silicon oxides with high reaction rate. Spatially resolved photoemission analysis with submicron resolution has been utilized to study the oxidation states of converted silicon oxide patterns in comparison with the surrounding Si_3N_4 layer. The core level shift of the Si $2p$ photoelectron peak and the spectral features in the valence band reveal a complete conversion of silicon nitride to silicon oxide at a bias voltage of 10 V, with no remaining nitrogen left. The major oxide is SiO_2. The observed oxidation states of Si^{4+}, Si^{3+}, and Si^{2+} show a gradient depth distribution indicating excess silicon in the layer. *© 2001 American Institute of Physics.* [DOI: 10.1063/1.1415415]

The need for lithographic techniques with nanometer spatial resolution is obvious for the development of new quantum devices and molecular electronics. In the recent decade, scanned probe microscopy, such as scanning tunneling microscopy (STM) or atomic force microscopy (AFM) has emerged as an important tool in nanoscale device fabrication by utilizing the effect that a local high electrical field between the probing tip and sample can modify the surface chemistry in a selective way with nanometer scale resolution. This has been demonstrated for the AFM-induced anodic oxidation in air of Si,[1,2] metal surfaces[3] and insulating thin films,[4] as well as for the hydrogen-terminated Si surfaces by ultrahigh vacuum (UHV) STM-induced hydrogen bond breaking, and subsequent reaction with various molecules.[5,6] The recently reported nanoscale conversion of silicon nitride film to silicon oxide by one of the authors (S.G.) showed an amazingly high reaction rate,[7] compared with the case of thermal oxidation.[8] It is widely accepted that the mechanism for the process of Si anodic AFM oxidation in regular atmosphere at room temperature is essentially controlled by air humidity, i.e., the adsorption of water on the surface. Negatively charged oxygen ions are injected from the water, and under the high electric field, oxyanions are transported through the oxide layer to the Si/SiO_2 interface, where they react with the positively charged holes and Si to form SiO_2. The oxide density is shown to be sensitive to voltage pulse parameters and substrate doping.[9] Space charge effects associated with defect generation during growth are responsible for nonuniformity of the oxide. In the case of Si_3N_4 conversion, the reaction between oxyanions, silicon nitride, and the holes accumulated at the Si_3N_4/oxide interface causes a replacement of nitrogen by oxygen. How far and under what condition Si_3N_4 film can be completely converted to SiO_2 or only partially into $SiO_{x<2}$ or SiO_xN_y is the subject of this letter and essential for understanding the silicon nitride oxidation mechanism. The conversion to $SiO_{x<2}$ would imply the coexistence of Si–O and Si–Si bonds in the oxide layer due to an excess of Si. Previous micro-Auger electron spectroscopy measurements of AFM-induced oxide pads on Si_3N_4 film showed the disappearance of the N-*KLL* peak and an enhancement of the O-*KLL* signal.[4,7] This indicates that the conversion to oxynitrides with a substantial amount of nitrogen in the layer is insignificant. Auger electron spectroscopy in this case, however, can only reveal elemental composition but cannot distinguish between chemical states. Photoelectron spectroscopy is known for chemical sensitivity, but generally has a lack of spatial resolution in the conventional mode of operation. We have utilized one of the few available systems in the world to perform spatially resolved photoemission experiments[10] with submicron resolution to study pads of AFM-converted silicon oxide patterned on Si_3N_4 film.

The silicon nitride films were grown on p-type Si(001) wafers with the low pressure chemical vapor deposition technique.[7] The original film thickness was 50 Å, which was then reduced to about 25 Å by HF (1%) etching to guarantee the complete oxidation of the Si_3N_4 film. Local field-induced

[a]Author to whom correspondence should be addressed; electronic mail: klauser@srrc.gov.tw
[b]Also with: Institute of Atomic and Molecular Sciences, Academia Sinica, Taipei 106, Taiwan, Republic of China.

Downloaded 31 Oct 2001 to 210.241.28.12. Redistribution subject to AIP license or copyright, see http://ojps.aip.org/aplo/aplcr.jsp

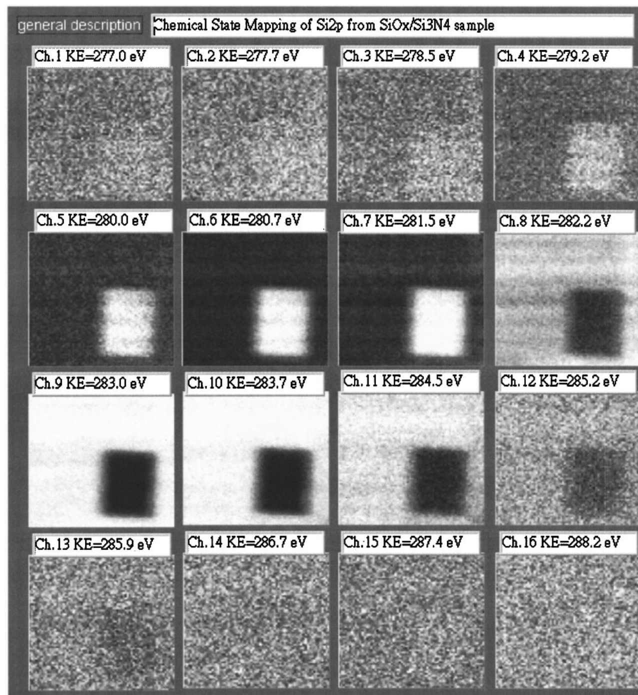

FIG. 1. 16 simultaneously acquired scanning photoemission microscopy images of Si $2p$ photoelectrons at different kinetic energies from an 8 μm$\times$10 μm pad of AFM-oxidized Si_3N_4 film (image size: 21 μm$\times$21 μm, photon energy: 384 eV).

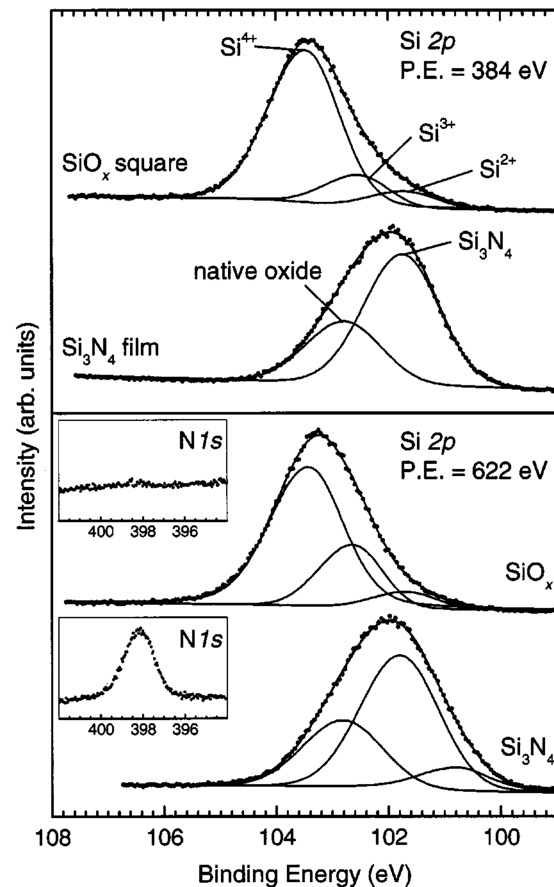

FIG. 2. Microphotoemission spectra (dotted curves) and peak analysis of Si $2p$ on the Si_3N_4 film and inside the AFM-oxidized pad. Insets are the corresponding N $1s$ spectra.

oxidation was performed in air atmosphere with a commercial AFM system using conductive PtIr-coated probes. The applied bias voltages were between 7 and 10 V, producing various patterns of stripes and pads. For locating the pattern on the sample, however, large squares 8 μm$\times$10 μm were often used in this study. Without any further surface treatment, the samples were imaged in a UHV chamber by soft x-ray scanning photoemission microscopy (SPEM). This custom-made apparatus at the Synchrotron Radiation Research Center in Hsinchu, Taiwan is based on focusing a soft x-ray beam in the range between 250 and 800 eV from an undulator beamline by means of Fresnel zone plate optics onto a spot 0.1 μm in size.[11] Details of the SPEM design and performance were given previously.[10,11] The overall spatial resolution in this experiment is 0.2 μm.

Figure 1 shows a set of 16 simultaneously acquired photoemission images for a photon energy (PE) of 384 eV and the photoelectron binding energy (BE) between 96 and 108 eV, where the Si $2p$ peak is located. The pad size of AFM-oxidized Si_3N_4 film (bias voltage of 10 V) is 8 μm$\times$10 μm. The gray scale reflects the intensity of the photoelectrons. Obviously, the oxidized pattern can be clearly distinguished. The Si $2p$ signal inside the pad is maximal at channel 7, representing the state of silicon oxide. Channel 9, with 1.5 eV higher kinetic energy than channel 7, shows reversed contrast and reflects the second chemical state of Si, i.e., Si_3N_4. Channels of background intensity far beyond the peak signal (channels 1–4 and 13–16) reveal very little contrast. The topographic height difference between the oxide pattern and Si_3N_4 is too small (the protruded oxide is about 60% of the Si_3N_4 film thickness[4]) to become evident in the SPEM image. Similar SPEM maps as for Si $2p$ can be obtained for the energy ranges of N $1s$ and O $1s$ core levels.

From the imaging mode, one can switch to the spectroscopic mode for micro-ultraviolet or micro-x-ray photoelectron spectroscopy analysis by selecting a particular point on the image and measuring photoemission energy distribution curves. This is displayed in Fig. 2 for a point near the center of the oxidized pad and for two different photon energies. The photon energy has been calibrated by the Fermi edge of a gold sample attached to the same sample holder. Avoiding the possible calibration error due to charging, the binding energy scale has also been determined by the carbon contamination of the samples. After subtraction of the secondary electron background, the Si $2p$ spectra were fitted by doublets of Voigt function with a standard spin-orbit splitting and branching ratio of the Si $2p_{3/2}$ and Si $2p_{1/2}$ peak constituents of 0.61 eV and 2, respectively. The Si $2p$ spectra of the silicon oxide pad for both photon energies show a clear asymmetry to lower BE. The three deconvoluted components have Si $2p_{3/2}$ peak maxima at 103.3, 102.4, and 101.6 eV with full-width-at-half-maximum (FWHM) of 1.3, 1.1, and 1.1 eV, respectively. The BE and the width of the major component agree well with reference values found in the literature for SiO_2.[12] Si $2p$ core-level spectroscopy of thermally grown SiO_2 film on Si(100) and Si(111) surfaces exhibits four oxidation states of silicon. Besides $SiO_2(Si^{4+})$, intermediate states of $Si^{1+}(Si_2O)$, $Si^{2+}(SiO)$, and $Si^{3+}(Si_2O_3)$ exist at the SiO_2/Si interface. The energy positions of the two deconvoluted shoulder peaks of the SiO_x square in Fig. 2 relative to the SiO_2 peak agree with the

Downloaded 31 Oct 2001 to 210.241.28.12. Redistribution subject to AIP license or copyright, see http://ojps.aip.org/aplo/aplcr.jsp

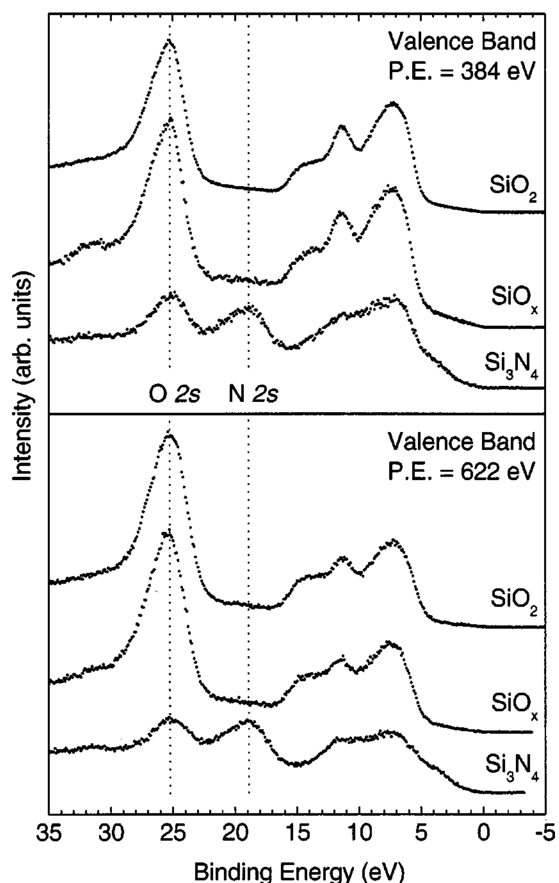

FIG. 3. Valence band spectra on the Si_3N_4 film, inside the AFM-oxidized pad, and of a 60 Å thick SiO_2 reference sample (thermally oxidized). Energy zero point corresponds to the Fermi edge of an Au reference sample.

suboxides Si^{3+} and Si^{2+} for the thermally oxidized Si film, but with about 20% larger peak widths. The Si^{3+} species increases in intensity for larger probing depth at photon energy of 622 eV (the electron escape length at PE=384 eV is about 10 Å and at PE=622 eV is about 14 Å), whereas the Si^{2+} suboxide intensity remains small. We conclude that those chemical states are due to intermediate oxides produced by the AFM-induced conversion of Si_3N_4, but with no remaining nitrogen incorporated in the film as indicated by the absence of N 1*s* (insert in Fig. 2) and N 2*s* (Fig. 3) signals. The silicon oxide pad is by about 1.5 nm thicker than the nitride film because of the additional protrusion. The suboxides can therefore not directly originate from the SiO_2/Si interface, but from an extended area in the layer containing excess Si–Si bonds.

The Si 2*p* peak of Si_3N_4 film is quite broad with contributions from stoichiometric Si_3N_4 with Si $2p_{3/2}$ peak maximum at 101.6 eV and from native oxide contamination at the surface with the corresponding peak at 102.6 eV. For PE =622 eV, additional contributions from Si at the Si_3N_4/Si interface with 100.7 eV BE is also evident. The difference between SiO_2 and the oxygen contamination of Si_3N_4 film also appears in the binding energy values of O 1*s* with 533.2 eV for silicon dioxide and 532.8 eV for native oxide. Both the N 1*s* signal with maximum intensity at 398.1 eV BE and the fitted Si $2p_{3/2}$ peak at 101.6 eV have FWHM of 1.4 eV, as expected for a well-prepared Si_3N_4 film. Figure 3 shows the valence band spectra of a silicon nitride film, the AFM-oxidized pad, and a 60 Å thick reference sample of thermal SiO_2 for two different photon energies. The main contributions in these spectra between 15 and 35 eV are from O 2*s* and N 2*s*, and those below 15 eV are mostly from Si 3*s*, Si 3*p*, O 2*p*, and N 2*p*. The AFM-induced oxidation results in a strong increase in O 2*s* intensity and the absence of N 2*s* signal. The band edge and the shape of the valence band resemble the spectrum of thermal dioxide. However, a slight increase in background intensity between 1 and 4 eV illustrates the presence of excess silicon in the layer. The band offset between 60 Å SiO_2 and Si_3N_4 film is about 4.0 eV. This value can be compared with 1.5 eV, measured by hole injection in Si_3N_4.[13] We can assume that this inconsistency can be related to the existence of the silicon-rich oxynitride phase at the Si_3N_4/native oxide interface, which was previously observed.[8]

In summary, spatially resolved soft x-ray photoemission microscopy has been employed to study AFM-induced oxidation on silicon nitride films. This technique provides direct evidence of the oxidation state distribution. It is found that a well-prepared sample can be completely converted to silicon oxide. The major oxide is SiO_2. Within the probing depth of the photoelectrons, other oxidation states of Si^{3+} and Si^{2+} are also observed. Apparently, suboxides containing Si–Si bonds are produced in the layer with gradient depth distribution. Excess Si in the layer escaping from the Si_3N_4/oxide interface might explain the enhancement of the oxidation reaction.

The authors acknowledge Dr. T.-S. Chao of National Nano Device Laboratory for supplying the Si_3N_4 and SiO_2 samples. This work is supported by the National Science Council of ROC and the Ministry of Education.

[1] J. A. Dagata, J. Schneir, H. H. Harary, C. J. Evans, M. T. Postek, and J. Bennett, Appl. Phys. Lett. **56**, 2001 (1990).
[2] M. Calleja, J. Anguita, R. Garcia, K. Birklund, F. Perez-Murano, and J. A. Dagata, Nanotechnology **10**, 34 (1999).
[3] E. S. Snow and P. M. Campbell, Science **270**, 1639 (1995).
[4] F. S.-S. Chien, J.-W. Chang, S.-W. Lin, Y.-C. Chou, T. T. Chen, S. Gwo, T.-S. Chao, and W.-F. Hsieh, Appl. Phys. Lett. **76**, 360 (2000).
[5] T.-C. Shen, C. Wang, J. W. Lyding, and J. R. Tucker, Appl. Phys. Lett. **66**, 976 (1995).
[6] M. C. Hersam, N. P. Guisinger, and J. W. Lyding, Nanotechnology **11**, 70 (2000).
[7] F. S.-S. Chien, Y.-C. Chou, T. T. Chen, W.-F. Hsieh, T.-S. Chao, and S. Gwo, J. Appl. Phys. **89**, 2465 (2001).
[8] V. A. Gritsenko, S. N. Svitasheva, I. P. Petrenko, H. Wong, J. B. Xu, and I. H. Wilson, J. Electrochem. Soc. **146**, 780 (1999).
[9] K. Morimoto, F. Perez-Murano, and J. A. Dagata, Appl. Surf. Sci. **158**, 205 (2000).
[10] C.-H. Ko, R. Klauser, D.-H. Wei, H.-H. Chan, and T. J. Chuang, J. Synchrotron Radiat. **5**, 299 (1998).
[11] I.-H. Hong, T.-H. Lee, G.-C. Yin, D.-H. Wei, J.-M. Juang, T.-E. Dann, R. Klauser, T. J. Chuang, C. T. Chen, and K.-L Tsang, Nucl. Instrum. Methods Phys. Res. A **905**, 467 (2001).
[12] F. J. Himpsel, F. R. McFeely, A. Taleb-Ibrahimi, J. A. Yarmoff, and G. Hollinger, Phys. Rev. B **38**, 6084 (1988).
[13] V. A. Gritsenko, E. E. Meerson, and Yu. N. Morokov, Phys. Rev. B **57**, R2081 (1998).

Downloaded 31 Oct 2001 to 210.241.28.12. Redistribution subject to AIP license or copyright, see http://ojps.aip.org/aplo/aplcr.jsp